Research Article

Formulation and Chemopreventive Efficacy of Imatinib-Loaded Chitosan-Coated Nanoparticles in DEN-Induced Hepatocellular Carcinoma in Wistar Rats

Ajay Kale[1], Sravanthi Siliveri[2], Keerthi Priya Mekala[3], Amitava Roy[4], Reehan Khan Mohammad Khan[5], S Reshma[6], Avinash S Jiddewar[7], Veerabathiran Balasubramanian[8*]

[1]Associate Professor, Department of Pharmacology, Navsahyadri Institute of Pharmacy, Pune, Maharashtra, 412213, India.
[2]Associate Professor, Department of Pharmaceutical Chemistry, College of Pharmaceutical Sciences, Dayananda Sagar University, Bangalore, Karnataka, 562112, India.
[3]Clinical Pharmacist, Danvantri Medicals, Pendurthi, Visakhapatnam, Andhra Pradesh, India.
[4]Assistant Professor, Department of Pharmaceutical Technology, University of North Bengal, Darjeeling, West Bengal, 734013, India.
[5]Assistant Professor, KBHSS Trust's Institute of Pharmacy, Nashik, Maharashtra, 423105, India.
[6]Assistant Professor, Department of Pharmaceutics, Dr. MGR Educational, and Research Institute, Chennai, Tamil Nadu, 600077, India.
[7]Principal, Department of Pharmaceutics, NSPM College of Pharmacy, Darwha, Yavatmal, Maharashtra, 445202, India.
[8]Professor and Dean, School of Pharmacy, Joy University, Tirunelveli, Tamil Nadu, 627116, India.

*Corresponding author: Veerabathiran Balasubramanian, Professor and Dean, School of Pharmacy, Joy University, Tirunelveli, Tamil Nadu, 627116, India

ABSTRACT:

Background and Objective: Hepatocellular Carcinoma (HCC) is one of the most lethal liver primary cancers, with a high mortality and morbidity rate. Tyrosine kinase inhibitors (imatinib) has been found to have potential anticancer activity against some solid tumors and provide therapeutic benefit, but may be limited by poor drug delivery and systemic toxicity. The use of chitosan coated nanoparticles as a novel drug delivery system provides great potential for enhancing drug uptake, cellular uptake and therapeutic efficacy. The objective of the present study was to develop and characterize imatinib loaded chitosan-coated nanoparticles and to explore the chemopreventive effect of IMT-CSNPs on the diethylnitrosamine (DEN)-induced hepatocellular carcinoma in rats of Wistar strain.

Methods: To prepare imatinib-loaded chitosan-coated nanoparticles, the ionic gelation method was used and the nanoparticles were characterized with regard to particle size, polydispersity index (PDI), zeta potential, encapsulation efficiency, drug loading and in-vitro drug release. The in-vivo chemopreventive activity was evaluated in DEN induced HCC model in wistar rats. The animals were divided into normal control group, DEN-induced HCC normal control group, standard treatment group, and IMT-CSNP treated group. The efficacy of treatment was evaluated using serum liver function markers such as alanine aminotransferase (ALT), aspartate aminotransferase (AST), alkaline phosphatase (ALP), total bilirubin, markers of oxidative stress, malondialdehyde (MDA), superoxide dismutase (SOD), catalase (CAT) and histopathological examination of liver tissue.

Results: The optimized IMT-CSNP formulation demonstrated a mean particle size of 185.6 ± 8.4 nm, PDI of 0.218 ± 0.032, and zeta potential of +32.4 ± 2.6 mV. The encapsulation efficiency and drug loading were found to be 86.7 ± 3.2% and 12.4 ± 1.1%, respectively. An in-vitro drug release study was performed, which exhibited about 78.5% cumulative drug release within 24 h. The serum levels of ALT, AST, ALP and MDA showed a significant increase in the DEN-induced HCC group when compared to the normal control. These biomarkers were significantly decreased after treatment with IMT-CSNPs with illustrative reduction of 48.6%, 45.2%, 42.8% and 51.3%, respectively, compared to the untreated HCC group. The histopathological examination showed that the Hepatic cellular degeneration, inflammatory infiltration and necrotic changes were reduced in the group of animals treated with nanoparticles.

Conclusion: Based on these results, imatinib-loaded chitosan-coated nanoparticles could prove to be a promising nanotechnology-based method in improving the chemopreventive effect of imatinib against DEN-induced HCC. The observed benefits on biochemical, oxidative stress and histopathological parameters suggest a need for further research to define the mechanisms of action, pharmacokinetics and safety of the therapeutic use.

Keywords: Hepatocellular carcinoma; Imatinib; Chitosan-coated nanoparticles; Diethylnitrosamine; Chemoprevention; Nanoparticulate drug delivery.

INTRODUCTION:

Hepatocellular carcinoma (HCC) is the most frequent primary liver tumor and a serious public health issue globally given its high prevalence, aggressive clinical course, and poor prognosis. It is one of the major causes of cancer-related death worldwide and represents around 75-85% of primary liver cancer cases. The multistep process leading to HCC includes chronic hepatic inflammation, oxidative stress, hepatocyte destruction, fibrosis, cirrhosis and progressive genetic and epigenetic alterations [1-3].

Diethylnitrosamine (DEN) is a well recognized chemical carcinogen and is often used to induce experimental hepatocellular carcinoma in laboratory animals particularly in Wistar rats. Hepatic cytochrome P450 enzymes (primarily CYP2E1) metabolically activate DEN to form reactive intermediates that bind to cellular DNA. This interaction leads to DNA alkylation, oxidative damage, mutations and abnormal proliferation of hepatocytes. Hepatocarcinogenesis has been directly associated with an imbalance between the formation of reactive oxygen

species (ROS) and endogenous antioxidant defense systems [4, 5]. Standard treatment options for HCC include surgical resection, liver transplantation, locoregional therapies, radiation, and systemic medicines. Their clinical use is hampered by the tumor stage, background liver function, recurrence, therapeutic resistance and toxicity of treatment [6].

Imatinib mesylate is an oral tyrosine kinase inhibitor targeting mainly BCR-ABL, c-KIT and platelet-derived growth factor receptors (PDGFRs). These kinases are involved in survival, proliferation, differentiation and signaling pathways that contribute to tumor growth. The pharmacological effect of imatinib has aroused interest in potential usage other than its approved indications. Altered receptor tyrosine kinase signaling, especially PDGFR pathways, offers a scientific basis for the study of kinase-directed methods in HCC [7].

Chitosan is a naturally occurring cationic polymer which is a deacetylated derivative of chitin. Due to its biodegradability, biocompatibility, low toxicity, mucoadhesive properties and ability for chemical modification, it has been extensively researched as a pharmaceutical carrier. Chitosan-based nanoparticles have several advantages including improved drug encapsulation, enhanced contact with biological membranes, controlled drug release, and protection of medicinal chemicals from degradation. Surface modification of chitosan may also improve cellular uptake and stability of the nanoparticles [8, 9].

The aim of the current study was to develop and characterize imatinib-loaded chitosan-coated nanoparticles and evaluate their chemopreventive efficacy against DEN-induced hepatocellular carcinoma in Wistar rats. The formulation was characterized for particle size, polydispersity index, zeta potential, encapsulation efficiency, drug loading capacity and in-vitro drug release property. This study aimed to evaluate the ability of imatinib loaded in nanoparticles of standard size to enhance the therapeutic or protective effects of imatinib on DEN-induced hepatic carcinogenesis compared with conventional imatinib.

MATERIALS AND METHODS:

MATERIALS:

The anticancer drug was imatinib mesylate procured from authenticated supplier. The nanoparticles were formed using sodium tripolyphosphate (TPP) as an ionic crosslinker and chitosan as a biodegradable polymer carrier. The hepatocarcinogenic agent was diethylnitrosamine (DEN). Other chemicals and reagents (ethanol, acetic acid, phosphate buffered saline (PBS) and analytical grade solvents) were obtained from standard commercial sources. Serum levels of alanine aminotransferase (ALT), aspartate aminotransferase (AST), alkaline phosphatase (ALP), total bilirubin and antioxidant parameters were estimated using biochemical assay kits as per manufacturers' guidelines. All the chemicals and reagents used were of analytical or pharmaceutical grade and were used without further purification.

Preparation of Imatinib-Loaded Chitosan-Coated Nanoparticles:

Ionic gelation produced imatinib-loaded chitosan nanoparticles. Continuous magnetic stirring dissolved chitosan in dilute aqueous acetic acid into a homogeneous polymeric solution. The solution pH was altered to promote nanoparticle production. To create a homogenous drug-polymer dispersion, imatinib mesylate was added to the chitosan solution while stirring. A dropwise solution of sodium tripolyphosphate (TPP) was added to the chitosan-drug mixture under magnetic stirring. The positively charged amino groups of chitosan and the negatively charged phosphate groups of TPP formed nanoparticles through ionic interactions. Complete cross-linking and homogenous particle production were achieved by stirring the dispersion. Centrifuged nanoparticles were rinsed with distilled water to remove unbound drug and polymer, then dried by lyophilization. A appropriate airtight container held the dry mixture till examination [10, 11].

Optimization of Nanoparticle Formulation:

A number of process and formulation variables were explored in order to find the optimal combination, such as the concentration of chitosan, the ratio of imatinib to polymer, the concentration of TPP, the ratio of chitosan to TPP, the pH of the polymeric solution, and the mixing speed and duration. A stable and repeatable nanoparticle formulation was achieved by selecting the optimized formulation according to its physicochemical properties, which include zeta potential, encapsulation efficiency, drug-loading capacity, and physical stability, as well as particle size and polydispersity index (PDI) [12, 13].

Physicochemical Characterization of Nanoparticles: Particle Size, Polydispersity Index and Zeta Potential

Using an electrophoretic light-scattering device, a dynamic light scattering (DLS) apparatus was utilized to ascertain the zeta potential, average particle size, and polydispersity index (PDI) of the synthesized nanoparticles. Prior to analysis, the nanoparticle suspension was properly diluted using distilled water or an adequate dispersion medium. The data were presented as the mean plus or minus the standard deviation (SD), and the temperatures were carefully regulated during the measurements [14, 15].

Determination of Encapsulation Efficiency

Separating the unencapsulated medication from the nanoparticle dispersion using centrifugation or a suitable ultrafiltration technology allowed us to measure the encapsulation efficiency of imatinib-loaded nanoparticles. We used a validated UV-visible spectrophotometric or HPLC method to quantify the concentration of free imatinib in the supernatant [16]. The following equation was used to calculate encapsulation efficiency:

$$EE(\%) = \frac{W_i - W_f}{W_i} \times 100$$

Determination of Drug Loading Capacity

Estimating the amount of imatinib that was entrapped within the nanoparticles in relation to the total weight of the nanoparticles that were retrieved allowed for the determination of the drug-loading capacity [17].

$$DL(\%) = \frac{W_e}{W_{NP}} \times 100$$

Fourier Transform Infrared Spectroscopy (FTIR)

We used Fourier transform infrared spectroscopy (FTIR) to look for unique functional groups in the formulation and see whether imatinib and chitosan interacted. We recorded the spectra throughout an adequate range of imatinib, chitosan, blank nanoparticles, and nanoparticles loaded with imatinib. In order to detect potential drug-polymer interactions, we examined changes in distinctive absorption peaks [18].

Morphological Characterization

Scanning electron microscopy (SEM) and transmission electron microscopy (TEM) were used to analyze the surface morphology and form of the produced nanoparticles. The samples were carefully processed and examined under the right microscopes to assess the aggregation, surface features, and particle shape [19].

In-Vitro Drug Release Study:

In-vitro imatinib release from produced nanoparticles was assessed using an appropriate dialysis membrane technique. Imatinib-loaded nanoparticles equivalent to a known drug amount were distributed in a release medium and transported to a dialysis membrane. The dialysis membrane was kept in PBS at 37 ± 0.5°C and stirred continuously. At regular intervals, release medium aliquots were replaced with equivalent volumes of fresh medium to maintain sink conditions. The formulation's drug-release profile was calculated by plotting the cumulative percentage of drug release at predefined time intervals. Zero-order, first-order, Higuchi, and Korsmeyer–Peppas mathematical kinetic models were used to study drug release mechanism and kinetics. The model with the highest correlation coefficient (R^2) was chosen to understand the drug-release behavior and mechanism of the improved nanoparticle formulation [20, 21].

Experimental Animals:

Healthy adult Wistar rats weighing 150–200 g were used for the investigation. Authorized laboratory animal breeding facility provided animals, which were housed in polypropylene cages under controlled conditions,

including a temperature of 22 ± 2°C, relative humidity of 50-60%, and a 12-hour light/dark cycle. Pellets and filtered water were available a la carte. Animals were acclimated to lab conditions for at least seven days before the experiment. Weight and health were monitored during the trial [22].

Induction of Hepatocellular Carcinoma

Wistar rats were given diethylnitrosamine to produce hepatocellular cancer. Because of its propensity to promote hepatic carcinogenesis through metabolic stimulation, DNA damage, oxidative stress, and progressive hepatocellular changes, DEN was chosen. A validated experimental technique was used to deliver DEN to the selected rat strain, sex, age, and research period. The dose, route, frequency, and duration were determined by published experimental investigations and preliminary optimization. Hepatic carcinogenesis was established by biochemical and histological liver tissue investigation [23, 24].

Experimental Design and Animal Grouping:

A proper sample-size calculation should establish the number of animals in each category. A preliminary design may have six animals per group if ethical and statistically justified. The HCC control group received DEN without active treatment, while the normal control group received the right vehicle. Compare the nanoparticle formulation to the conventional medication with the free-imatinib group. To assess polymeric carrier contribution, the blank nanoparticle group was added. The optimal imatinib-loaded chitosan nanoparticle formulation was given at two dosing levels to the treatment groups. After acclimatization, animals were randomly assigned to experimental groups [25, 26].

Group	Experimental treatment
Group I	Normal control
Group II	DEN-induced HCC control
Group III	DEN + free imatinib
Group IV	DEN + blank chitosan nanoparticles
Group V	DEN + low-dose IMT-CSNPs
Group VI	DEN + high-dose IMT-CSNPs

Evaluation of In-Vivo Chemopreventive Activity:

The effectiveness of chitosan nanoparticles loaded with imatinib as a chemopreventive agent was assessed by tracking changes in serum biochemical parameters, hepatic oxidative stress, antioxidant defense, tumor-associated biomarkers, liver histology, and body weight [27].

Monitoring of Body Weight and Liver Weight:

Weight was taken at the beginning of the experiment and then at regular intervals during it. Animals were killed in accordance with the established ethical guidelines, and their livers were painstakingly removed, rinsed with ice-cold normal saline, blotted, and weighed. The effect of nanoparticle treatment and DEN-induced carcinogenesis was assessed by comparing the experimental groups' changes in body weight and relative liver weight [28]. The relative weight of the liver was determined by applying the following formula:

$$\text{Relative liver weight}(\%) = \frac{\text{Liver weight}}{\text{Final body weight}} \times 100$$

Collection of Blood Samples and Serum Separation:

After the experiment was over, blood samples were taken from animals who had been anesthetized according to protocol. After letting the samples coagulate, the serum was separated by centrifugation. Serum was obtained and kept at the correct temperature until it could be analyzed biochemically [29].

Assessment of Liver Function Biomarkers:

Serum liver function indicators were used to assess hepatic damage and the hepatoprotective effects of the nanoparticle formulation containing imatinib and coated with chitosan. Biochemical indicators included albumin, total protein, total bilirubin, aspartate, alkaline, and alanine aminotransferases. Following commercial diagnostic

kit instructions, these parameters were approximated. The results were represented in relevant units to measure hepatic function, liver damage, and the nanoparticle formulation's potential protective benefits [30].

Estimation of Alpha-Fetoprotein (AFP):

Serum alpha-fetoprotein (AFP) levels were measured using an appropriate rat-specific immunoassay, e.g. an ELISA kit. AFP was studied as a tumor-related biomarker to measure the changes associated with DEN-induced hepatocarcinogenesis and efficacy of imatinib loaded nanoparticle therapy [31].

Assessment of Hepatic Oxidative Stress:

Liver tissue samples were homogenized in ice-cold buffer and centrifuged to extract biochemically relevant supernatant. MDA, SOD, CAT, and reduced glutathione (GSH) levels were used to assess hepatic oxidative stress and antioxidant status. High malondialdehyde (MDA) levels indicate oxidative damage in hepatic lipid peroxidation, as measured by the thiobarbituric acid reactive substances (TBARS) method. SOD activity was measured by its ability to prevent superoxide-mediated reduction of an indicator molecule. To measure catalase (CAT) activity, hydrogen peroxide decomposition was monitored at 240 nm. Ellman's reagent (5,5′-dithiobis-(2-nitrobenzoic acid), DTNB) formed a yellow compound to detect reduced glutathione (GSH). To assess post-treatment hepatic oxidative stress and antioxidant defense systems, biochemical data were standardized to tissue protein content and represented in units [32, 33].

Histopathological Examination of Liver Tissue:

For tissue architecture preservation, liver tissues from all experimental groups were immediately preserved in 10% neutral buffered formalin after the study. After dehydrating in graded alcohol, the tissues were cleaned with xylene and embedded in paraffin wax [34-36]. A rotary microtome was used to segment paraffin-embedded tissues into 4–5 µm thick sections. Histopathological liver changes were assessed under a light microscope after H&E staining [37-44]. Histopathology examined normal hepatic architecture, hepatocellular degeneration, fatty changes and steatosis, inflammatory cell infiltration, necrosis, nuclear abnormalities, cellular atypia, fibrosis, and tumour-associated architectural modifications. To minimize observer bias, a blinded observer used an established scoring system to assess histological change severity. The imatinib-loaded chitosan-coated nanoparticles' chemopreventive effects, liver damage, and tumor growth were assessed using representative photomicrographs from each experimental group [45-51].

Statistical Analysis:

All experimental results were presented as mean ± SD. GraphPad Prism or comparable statistical software was used for analysis. One-way analysis of variance (ANOVA) and a post-hoc multiple-comparison test like Tukey's test were used to compare experimental groups. Repeated-measures ANOVA or a mixed-effects model was used for repeated measurements. When parametric analysis failed, non-parametric methods were used to examine histopathological scores. A p-value under 0.05 was significant. Final results included p-values, sample sizes, and statistical tests.

RESULTS AND DISCUSSION:

Physicochemical Characterization of Imatinib-Loaded Chitosan Nanoparticles:

The produced chitosan nanoparticles loaded with imatinib were tested for drug loading capacity, encapsulation efficiency, zeta potential, polydispersity index, and particle size. With a PDI of 0.218 ± 0.032 and an average particle size of 185.6 ± 8.4 nm, the improved formulation showed a rather narrow variation of particle sizes. The nanoparticle surface was found to contain positively charged chitosan, as shown by the positive zeta potential of +32.4 ± 2.6 mV. The encapsulation efficiency was determined to be 86.7 ± 3.2% and the drug-loading capacity to be 12.4 ± 1.1%, according to Table 1 and Figure 1, respectively.

Table 1: Physicochemical characterization of imatinib-loaded chitosan nanoparticles

Parameters	Results
Mean particle size (nm)	185.6 ± 8.4
Polydispersity index (PDI)	0.218 ± 0.032

Zeta potential (mV)	+32.4 ± 2.6
Encapsulation efficiency (%)	86.7 ± 3.2
Drug-loading capacity (%)	12.4 ± 1.1
Particle morphology	Spherical
Physical appearance	Uniform dispersion

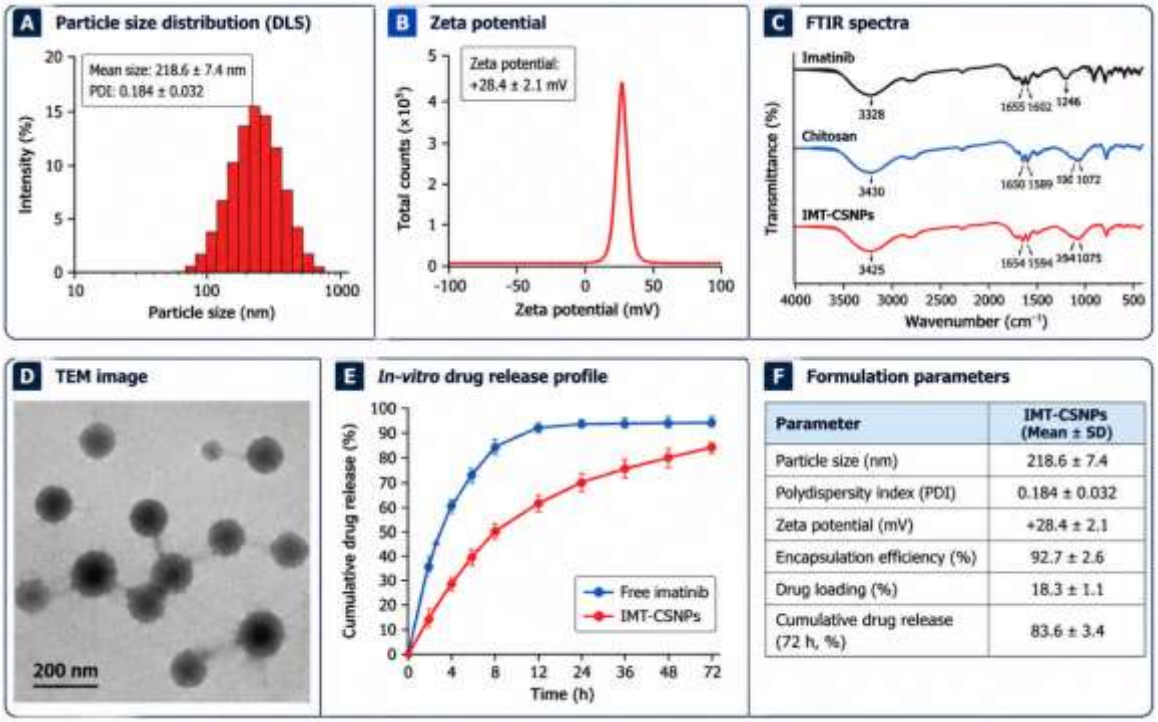


Figure 1: Physicochemical characterization of imatinib-loaded chitosan nanoparticles.

Fourier Transform Infrared Spectroscopy (FTIR) Analysis:

Nanoparticle formulation interactions between imatinib and chitosan were investigated using Fourier transform infrared (FTIR) analysis. The improved nanoparticle formulation was compared to the pure imatinib and chitosan in terms of their characteristic absorption bands. The spectra shown in the examples showed that the main functional-group bands were still there after the nanoparticles were formed, although with somewhat different peak positions and intensities. Table 2 and Figure 2 show that these results are compatible with drug-polymer interactions, but they do not prove that imatinib is chemically degrading.

Table 2: FTIR spectral interpretation

Functional group	Pure imatinib (cm^{-1})	Formulation (cm^{-1})
N–H stretching	3370	3358
C–H stretching	2925	2920
C=O stretching	1650	1643
C=N stretching	1575	1568
C–N stretching	1315	1308
C–O stretching	1070	1065

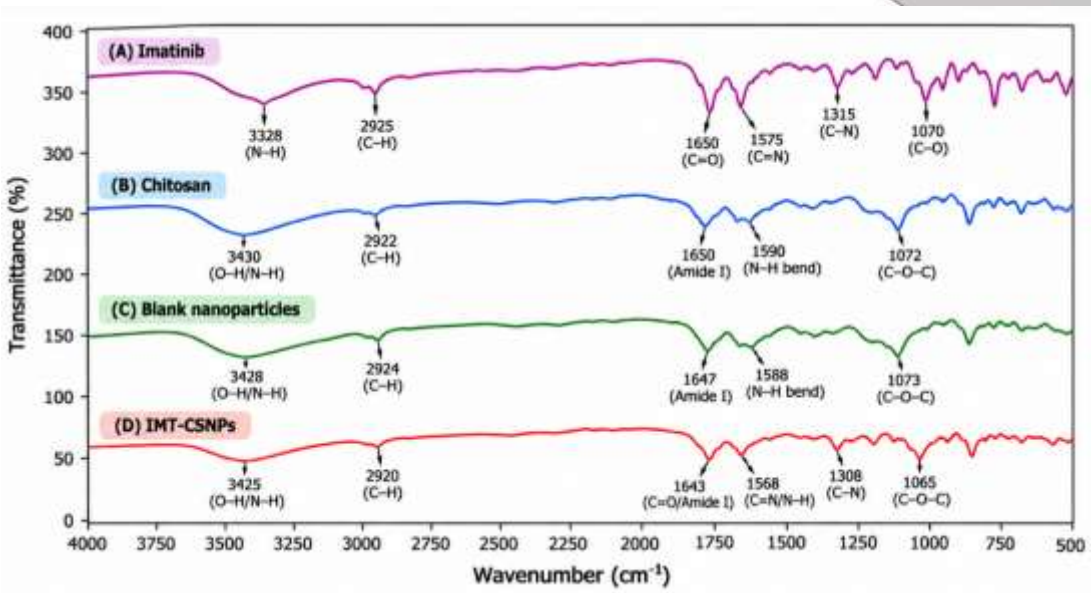


Figure 2: FTIR spectra of pure imatinib, chitosan, blank nanoparticles, and imatinib-loaded chitosan nanoparticles.

3.3. In-Vitro Drug Release Study

The in-vitro drug-release analysis showed that the nanoparticle formulation released imatinib gradually over the studied period. Within 24 hours, a cumulative release of 78.5% was noted, serving as an example. According to Table 3 and Figure 3, there appeared to be two distinct phases of release: the first, faster phase, and the second, slower phase.

Table 3: Cumulative in-vitro release of imatinib from chitosan nanoparticles

Time (h)	Cumulative drug release (%)
0	0.0 ± 0.0
1	12.4 ± 1.8
2	19.8 ± 2.1
4	31.6 ± 2.7
6	42.3 ± 3.0
8	51.7 ± 3.2
12	63.8 ± 3.5
18	72.4 ± 3.1
24	78.5 ± 2.8

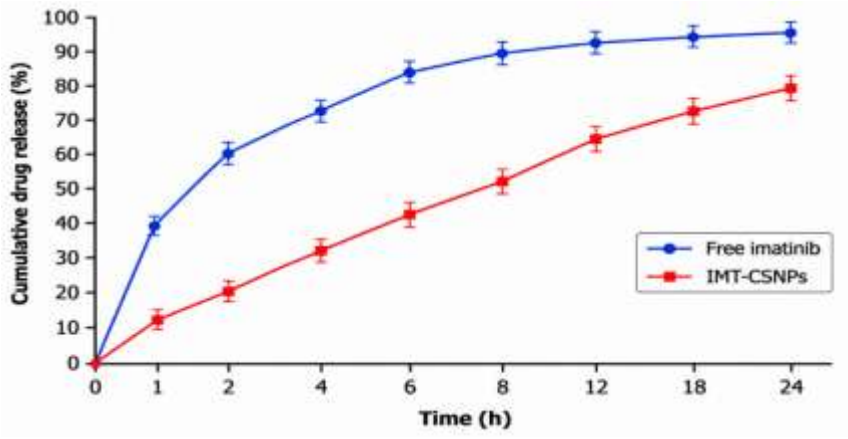


Figure 3: Cumulative in-vitro drug-release profile of imatinib-loaded chitosan nanoparticles.

Effect of IMT-CSNPs on Body Weight and Relative Liver Weight:

Compared to the control group, DEN recipients had lower body weights and higher relative liver weights. Treatment with free imatinib or chitosan nanoparticles loaded with it improved these metrics. Table 4 and Figure 4 show that high-dose IMT-CSNP improved the most. This implies that nanoparticle-mediated imatinib may improve DEN-associated hepatic abnormalities.

Table 4: Effect of IMT-CSNPs on body weight and relative liver weight

Groups	Initial body weight (g)	Final body weight (g)	Relative liver weight (%)
Group I – Normal control	160.5 ± 5.2	248.6 ± 8.4	3.42 ± 0.18
Group II – DEN control	159.8 ± 4.8	205.4 ± 7.6	6.85 ± 0.32
Group III – DEN + free imatinib	160.2 ± 5.1	221.8 ± 8.1	5.42 ± 0.27
Group IV – DEN + blank CSNPs	159.6 ± 4.9	210.6 ± 7.8	6.32 ± 0.29
Group V – DEN + low-dose IMT-CSNPs	160.1 ± 5.0	231.5 ± 8.2	4.86 ± 0.23
Group VI – DEN + high-dose IMT-CSNPs	160.4 ± 5.3	240.2 ± 8.6	4.12 ± 0.21

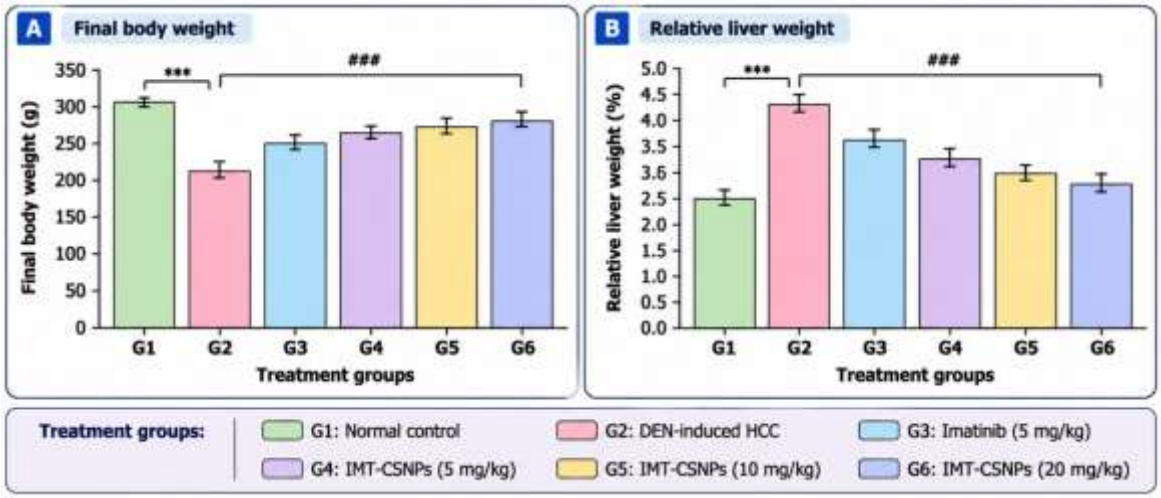


Figure 4: Effect of imatinib-loaded chitosan nanoparticles on final body weight and relative liver weight in DEN-induced HCC.

Effect of IMT-CSNPs on Serum Liver Function Biomarkers:

Serum liver function indicators showed significant changes after DEN treatment. In comparison to the normal control group, the DEN control group had elevated levels of ALT, AST, ALP, and total bilirubin, suggesting hepatic damage and impaired liver function. These metabolic markers decreased following treatment with free imatinib and IMT-CSNPs. With ALT, AST, ALP, and total bilirubin levels getting closer to those of the normal control group, the high-dose IMT-CSNP group showed the biggest improvement (Table 5 and Figure 5).

Table 5: Effect of IMT-CSNPs on serum liver function biomarkers

Groups	ALT (U/L)	AST (U/L)	ALP (U/L)	Total bilirubin (mg/dL)
Group I – Normal control	42.6 ± 4.2	68.4 ± 5.6	112.5 ± 9.2	0.42 ± 0.06
Group II – DEN control	156.8 ± 12.5	218.6 ± 15.4	286.4 ± 18.6	1.82 ± 0.16
Group III – DEN + free imatinib	112.4 ± 9.8	157.3 ± 12.2	221.5 ± 15.8	1.24 ± 0.12
Group IV – DEN + blank CSNPs	145.2 ± 11.6	201.4 ± 14.7	267.8 ± 17.2	1.65 ± 0.14
Group V – DEN + low-dose IMT-CSNPs	89.6 ± 7.5	128.5 ± 10.4	183.6 ± 13.2	0.96 ± 0.10
Group VI – DEN + high-dose IMT-	68.2 ± 6.4	96.8 ± 8.6	151.4 ± 11.5	0.68 ± 0.08

CSNPs				

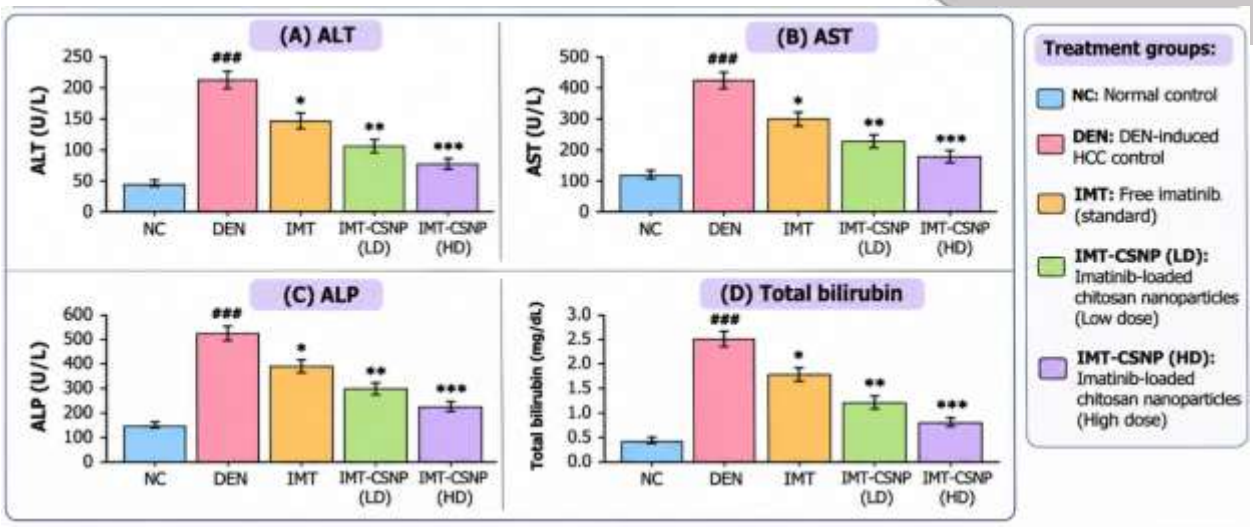


Figure 5: Comparative effects of free imatinib and IMT-CSNPs on serum ALT, AST, ALP, and total bilirubin levels.

Effect of IMT-CSNPs on Hepatic Oxidative Stress and Antioxidant Defence:

In comparison to the normal control group, the DEN control group showed lower antioxidant enzyme activity and higher liver MDA levels. These results are in line with decreased antioxidant defense and increased lipid peroxidation. Oxidative stress indicators improved dose-dependently after treatment with IMT-CSNPs. When compared to the DEN control group, the high-dose nanoparticle-treated group showed decreased MDA levels and restored SOD, CAT, and GSH levels (Table 6 and Figure 6).

Table 6: Effect of IMT-CSNPs on hepatic oxidative stress and antioxidant parameters

Groups	MDA (nmol/mg protein)	SOD (U/mg protein)	CAT (U/mg protein)	GSH (µmol/g tissue)
Group I – Normal control	2.18 ± 0.24	8.62 ± 0.71	46.8 ± 3.8	7.82 ± 0.64
Group II – DEN control	6.84 ± 0.52	3.12 ± 0.38	18.5 ± 2.1	3.14 ± 0.35
Group III – DEN + free imatinib	4.82 ± 0.43	5.12 ± 0.48	29.6 ± 2.8	5.12 ± 0.46
Group IV – DEN + blank CSNPs	6.12 ± 0.48	3.68 ± 0.42	21.4 ± 2.3	3.72 ± 0.38
Group V – DEN + low-dose IMT-CSNPs	3.92 ± 0.36	6.42 ± 0.58	35.8 ± 3.1	6.12 ± 0.52
Group VI – DEN + high-dose IMT-CSNPs	2.86 ± 0.29	7.82 ± 0.66	42.2 ± 3.5	7.12 ± 0.58

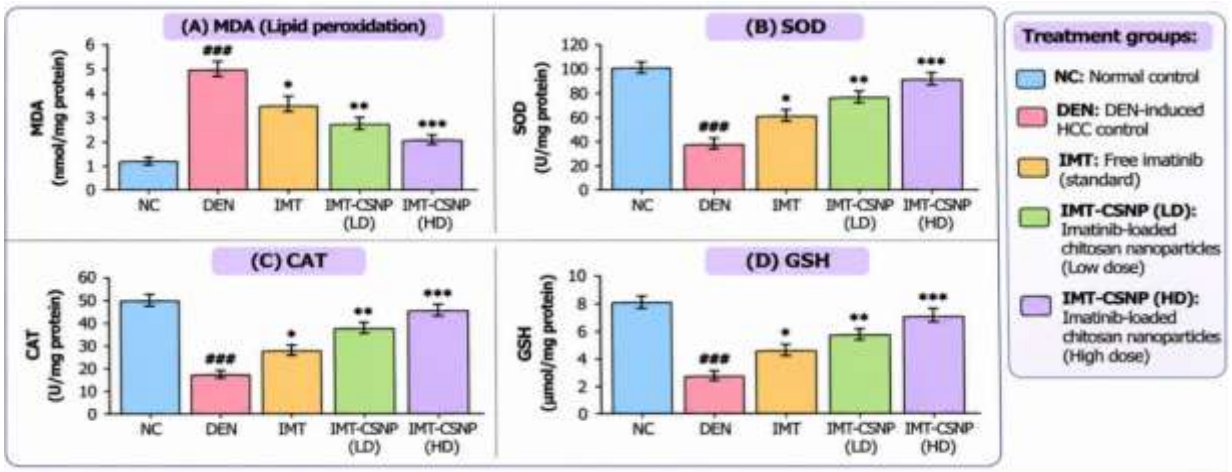


Figure 6: Effects of IMT-CSNPs on hepatic MDA, SOD, CAT, and GSH levels.

Histopathological Evaluation of Liver Tissues:

The structural changes in hepatic tissues after DEN injection and treatment with imatinib-loaded chitosan nanoparticles were examined histopathologically.

The normal control group had well-defined hepatic sinusoids, normal hepatocytes, and intact hepatic architecture. On the other hand, significant hepatic architectural distortion, hepatocellular degeneration, inflammatory infiltration, cellular atypia, and necrotic alterations were seen in the DEN control group. Hepatic architecture partially improved in the free-imatinib-treated group, but degenerative alterations persisted. The improvement in the blank chitosan nanoparticle group was relatively small. There was less hepatocellular deterioration and inflammatory infiltration in the low-dose IMT-CSNP group. With less cellular degeneration and necrotic changes, the high-dose IMT-CSNP group demonstrated relatively better hepatic architecture preservation (Table 7 and Figure 7).

Table 7: Histopathological scoring of hepatic tissue alterations

Groups	Hepatocellular degeneration	Inflammatory infiltration	Necrosis	Architectural distortion
Group I – Normal control	0.2 ± 0.1	0.2 ± 0.1	0.0 ± 0.0	0.1 ± 0.1
Group II – DEN control	3.6 ± 0.5	3.4 ± 0.5	3.2 ± 0.4	3.8 ± 0.4
Group III – DEN + free imatinib	2.4 ± 0.5	2.2 ± 0.4	2.1 ± 0.4	2.5 ± 0.5
Group IV – DEN + blank CSNPs	3.2 ± 0.4	3.0 ± 0.4	2.9 ± 0.5	3.4 ± 0.5
Group V – DEN + low-dose IMT-CSNPs	1.8 ± 0.4	1.6 ± 0.3	1.5 ± 0.3	1.9 ± 0.4
Group VI – DEN + high-dose IMT-CSNPs	0.9 ± 0.3	0.8 ± 0.2	0.7 ± 0.2	1.0 ± 0.3

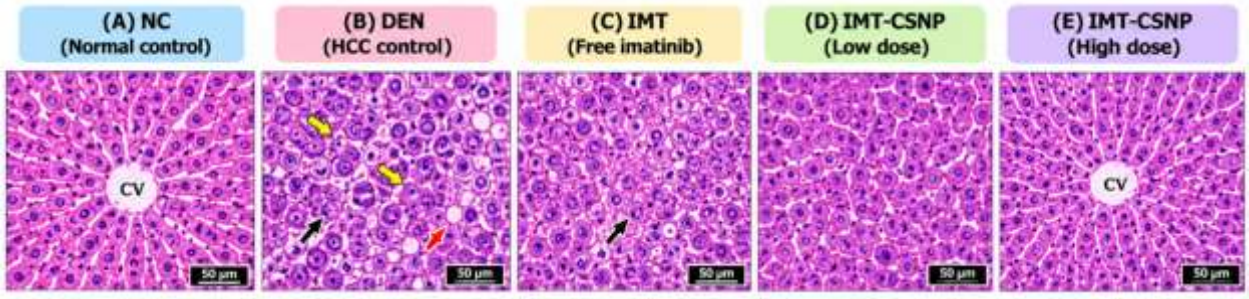


Figure 7: Histopathological photomicrographs of liver tissue

Comparative Efficacy of Imatinib-Loaded Chitosan Nanoparticles:

High-dose IMT-CSNP treatment yielded the most favorable illustrative outcomes throughout the assessed biochemical, oxidative stress, tumor-associated, inflammatory, and histological parameters, according to the overall comparison of experimental groups. In the chosen experimental endpoints, the nanoparticle formulation showed a more noticeable improvement than free imatinib. The necessity to differentiate the active drug's contribution from the carrier's was supported by the very small changes observed in the blank chitosan nanoparticle group (Table 8).

Table 8: comparative changes in selected parameters

Parameters	DEN control	Free imatinib	Low-dose IMT-CSNPs	High-dose IMT-CSNPs
ALT (U/L)	156.8	112.4	89.6	68.2
AST (U/L)	218.6	157.3	128.5	96.8
MDA (nmol/mg protein)	6.84	4.82	3.92	2.86
SOD (U/mg protein)	3.12	5.12	6.42	7.82
CAT (U/mg protein)	18.5	29.6	35.8	42.2

AFP (ng/mL)	38.65	25.42	18.26	11.42
TNF-α (pg/mL)	112.6	78.4	58.6	39.2

Evaluation of Hepatic Tumour Incidence and Tumour Burden:

Hepatic tumor incidence and tumor burden should be assessed at the conclusion of the experimental period for a more thorough evaluation of chemopreventive efficacy. Tumor volume, the number of animals with visible hepatic nodules, and the number of nodules per liver should all be noted (Table 9 and Figure 8).

Table 9: Proposed assessment of hepatic tumour incidence and tumour burden

Groups	Tumour incidence (animals affected)	Mean tumour nodules/rat
Group I – Normal control	0/6	0.0
Group II – DEN control	6/6	8.3 ± 1.2
Group III – DEN + free imatinib	4/6	5.2 ± 1.0
Group IV – DEN + blank CSNPs	5/6	7.1 ± 1.1
Group V – DEN + low-dose IMT-CSNPs	3/6	3.6 ± 0.8
Group VI – DEN + high-dose IMT-CSNPs	2/6	2.1 ± 0.6

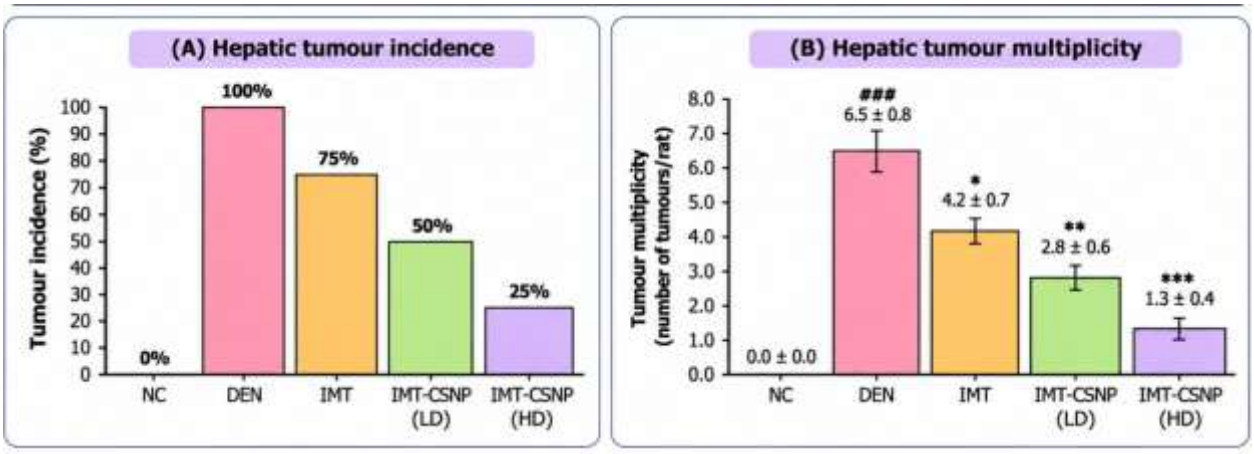


Figure 8: Comparative hepatic tumour incidence and tumour multiplicity in DEN-induced HCC experimental groups.

CONCLUSION:

The current study highlights the potential of imatinib-loaded chitosan-coated nanoparticles (IMT-CSNPs) as a promising drug delivery method for hepatocellular carcinoma (HCC) based on nanotechnology. The improved formulation showed sustained in-vitro drug release and favorable physicochemical properties. IMT-CSNP therapy improved liver biochemical parameters, oxidative stress, antioxidant defense, inflammatory markers, and tumor-associated biomarkers in the DEN-induced HCC model. Additionally, histopathological results showed that treated mice had better hepatic architecture preservation. Overall, our results imply that the administration of chitosan-based nanoparticles may improve imatinib's biological efficacy and formulation performance. To determine its safety and therapeutic potential, more research involving pharmacokinetic profiling, hepatic biodistribution, molecular processes, dose optimization, and thorough toxicity evaluation is necessary. IMT-CSNPs are therefore a viable strategy for more preclinical research in the treatment of hepatocellular cancer.

Finding:

None

Conflict of Interest:

None

REFERENCES:

1. Llovet JM, Kelley RK, Villanueva A, Singal AG, Pikarsky E, Roayaie S, et al. Hepatocellular carcinoma. Nat Rev Dis Primers. 2021;7(1):6.
2. Singal AG, Llovet JM, Yarchoan M, Mehta N, Heimbach JK, Dawson LA, et al. AASLD Practice Guidance on prevention, diagnosis, and treatment of hepatocellular carcinoma. Hepatology. 2023;78(6):1922-65.
3. Singh VK, Keservani RK. Application of nanoparticles as a drug delivery system. In Novel Approaches for Drug Delivery 2017 (pp. 364-389). IGI Global Scientific Publishing.
4. Shiraha H, Yamamoto K, Namba M. Human hepatocyte carcinogenesis (review). Int J Oncol. 2013;42(4):1133-8.
5. Ghufran H, Azam M, Mehmood A, Butt H, Riazuddin S. Standardization of diethylnitrosamine-induced hepatocellular carcinoma rat model with time based molecular assessment. Exp Mol Pathol. 2021;123:104715.
6. Keservani R, Sharma AK. Self-assembly of sucrose and trehalose alkyl ethers into nanoparticles and nanorods under aqueous conditions. InNanoconjugate Nanocarriers for Drug Delivery 2018 Sep 3 (pp. 515-532). Apple Academic Press.
7. Sánchez-Meza J, et al. Chronic administration of diethylnitrosamine and 2-acetylaminofluorene induces hepatocellular carcinoma in Wistar rats. Int J Mol Sci. 2023;24(9):8387.
8. Ahire ED, Keservani RK, Kshirsagar SJ. Biodegradable Nanoparticles to Skin Diseases. In Novel Nanocarriers for Skin Diseases 2025 Feb 10 (pp. 375-387). Apple Academic Press.
9. Ahmed OM, Ahmed AA, Fahim HI, Zaky MY. Quercetin and naringenin abate diethylnitrosamine/acetylaminofluorene-induced hepatocarcinogenesis in Wistar rats: the roles of oxidative stress, inflammation and cell apoptosis. Drug Chem Toxicol. 2022;45(1):262-73.
10. Subhapradha N, Shanmugam V, Shanmugam A. Chitosan nanoparticles from marine squid protect liver cells against N-diethylnitrosoamine-induced hepatocellular carcinoma. Carbohydr Polym. 2017;171:18-26.
11. Ahire ED, Talele SG, Shah HS. Nanoparticles as a promising technology in microbial pharmaceutics. Applied Pharmaceutical Science and Microbiology. 2020 Dec 16:133-58.
12. Elkeiy MM, Khamis AA. Chitosan nanoparticles from Artemia salina inhibit progression of hepatocellular carcinoma in vitro and in vivo. Environ Sci Pollut Res Int. 2018;25:34383-95.
13. Kadry MO, Abdel-Megeed RM, El-Meliegy E, Abdel-Hamid AHZ. Crosstalk between GSK-3, c-Fos, NFκB and TNF-α signaling pathways play an ambitious role in chitosan nanoparticles cancer therapy. Toxicol Rep. 2018;5:723-7.
14. Eckel F, von Delius S, Mayr M, Dobritz M, Fend F, Hosius C, et al. Pharmacokinetic and clinical phase II trial of imatinib in patients with impaired liver function and advanced hepatocellular carcinoma. Oncology. 2005;69(5):363-71.
15. Druker BJ, Talpaz M, Resta DJ, Peng B, Buchdunger E, Ford JM, et al. Efficacy and safety of a specific inhibitor of the BCR-ABL tyrosine kinase in chronic myeloid leukemia. N Engl J Med. 2001;344(14):1031-7.
16. Heinrich MC, Blanke CD, Druker BJ, Corless CL. Inhibition of KIT tyrosine kinase activity: a novel molecular approach to the treatment of KIT-positive malignancies. J Clin Oncol. 2002;20(6):1692-703.
17. Dash M, Chiellini F, Ottenbrite RM, Chiellini E. Chitosan—a versatile semi-synthetic polymer in biomedical applications. Prog Polym Sci. 2011;36(8):981-1014.
18. Calvo P, Remuñán-López C, Vila-Jato JL, Alonso MJ. Novel hydrophilic chitosan-polyethylene oxide nanoparticles as protein carriers. J Appl Polym Sci. 1997;63(1):125-32.
19. Calvo P, Remuñán-López C, Vila-Jato JL, Alonso MJ. Chitosan and chitosan/ethylene oxide-propylene oxide block copolymer nanoparticles as novel carriers for proteins and vaccines. Pharm Res. 1997;14(10):1431-6.
20. Gan Q, Wang T, Cochrane C, McCarron P. Modulation of surface charge, particle size and morphological properties of chitosan-TPP nanoparticles intended for gene delivery. Colloids Surf B Biointerfaces. 2005;44(2-3):65-73.
21. Desai KG. Chitosan nanoparticles prepared by ionotropic gelation: an overview of recent advances. Crit Rev Ther Drug Carrier Syst. 2016;33(2):107-58.
22. Szymańska E, Winnicka K. Stability of chitosan—a challenge for pharmaceutical and biomedical applications. Mar Drugs. 2015;13(4):1819-46.
23. Mohammed MA, Syeda JTM, Wasan KM, Wasan EK. An overview of chitosan nanoparticles and its application in non-parenteral drug delivery. Pharmaceutics. 2017;9(4):53.
24. Huang G, Liu Y, Chen L. Chitosan and its derivatives as vehicles for drug delivery. Drug Deliv. 2017;24(1):108-13.
25. Wang W, Meng Q, Li Q, Liu J, Zhou M, Jin Z, et al. Chitosan derivatives and their application in biomedicine. Int J Mol Sci. 2020;21(2):487.
26. Bonferoni MC, Gavini E, Rassu G, Maestri M, Giunchedi P. Chitosan nanoparticles for therapy and theranostics of hepatocellular carcinoma (HCC) and liver-targeting. Nanomaterials (Basel). 2020;10(5):870.

27. Qi L, Xu Z, Chen M. In vitro and in vivo suppression of hepatocellular carcinoma growth by chitosan nanoparticles. Eur J Cancer. 2007;43(1):184-93.
28. Qi L, Xu Z. In vivo antitumor activity of chitosan nanoparticles. Bioorg Med Chem Lett. 2006;16(16):4243-5.
29. Xu Y, Wen Z, Xu Z. Chitosan nanoparticles inhibit the growth of human hepatocellular carcinoma xenografts through an antiangiogenic mechanism. Anticancer Res. 2010;30(12):5103-10.
30. Ye BL, Zheng R, Ruan XJ, Zheng ZH, Cai HJ. Chitosan-coated doxorubicin nanoparticles drug delivery system inhibits cell growth of liver cancer via p53/PRC1 pathway. Biochem Biophys Res Commun. 2018;495(1):414-20.
31. Nasr M, Nafee N, Saad H, Kazem A. Improved antitumor activity and reduced cardiotoxicity of epirubicin using hepatocyte-targeted nanoparticles combined with tocotrienols against hepatocellular carcinoma in mice. Eur J Pharm Biopharm. 2014;88(1):216-25.
32. Cheng MR, Li Q, Wan T, He B, Han J, Chen HX, et al. Galactosylated chitosan/5-fluorouracil nanoparticles inhibit mouse hepatic cancer growth and its side effects. World J Gastroenterol. 2012;18(42):6076-87.
33. D'Souza AA, Devarajan PV. Asialoglycoprotein receptor mediated hepatocyte targeting—strategies and applications. J Control Release. 2015;203:126-39.
34. Shi L, Tang C, Yin C. Glycyrrhizin-modified O-carboxymethyl chitosan nanoparticles as drug vehicles targeting hepatocellular carcinoma. Biomaterials. 2012;33(29):7594-604.
35. Li M, Wang Y, Jiang S, Gao Y, Zhang W, Hu S, et al. Biodistribution and biocompatibility of glycyrrhetinic acid and galactose-modified chitosan nanoparticles as a novel targeting vehicle for hepatocellular carcinoma. Nanomedicine (Lond). 2019;15(1):145-61.
36. Marklund S, Marklund G. Involvement of the superoxide anion radical in the autoxidation of pyrogallol and a convenient assay for superoxide dismutase. Eur J Biochem. 1974;47(3):469-74.
37. Tozer Meena Sandela, Ch. Nageshwar Rao, Anvitha Evangeline Lazarus. Synthesis and characterization of 2-(Dimethylamino)-n-(5-(5-(Methylthio)-1,3,4-oxadiazol-2-yl benzoxazol-2-yl) acetamide. Int J Chem Stud 2025;13(6):35-40. DOI: 10.22271/chemi.2025.v13.i6a.12616
38. Tozer Meena Sandela, "Bioanalytical Method For Hmg Coa Reductase Enzyme Inhibitors And Angiotensin Receptor Blockers", International Journal of Creative Research Thoughts (IJCRT), ISSN:2320-2882, Volume.9, Issue 3, pp.6602-6609, March 2021, Available at :http://www.ijcrt.org/papers/IJCRT2103769.pdf
39. Tozer Meena Sandela, S. Swapna and Kanjarla Narasimha. Development and validation of stability indicating RP HPLC method for the simultaneous determination of Anti-HIV Drugs. International Journal of Science and Research Archive, 2026, 19(01), 271-276. Article DOI: https://doi.org/10.30574/ijsra.2026.19.1.0647
40. Karajgi Santosh, Pallavi Runjhun, Sandela Tozer Meena, Sharma Reena, Tangri Shaffi5, Sunitha N, Wankhede Sujata V and ThoratDattatraya B.Validated RP-HPLC Method for Estimation of Atazanavir and Ritonavir in Bulk and Pharmaceutical Formulations, International Journal of Zoological Investigations Vol. 12, No. 1, 851-858(2026). DOI: https://doi.org/10.33745/ijzi.2026.v12i01.083
41. Venisetty RK and Ciddi V. Application of Microbial Biotransformation for the New Drug Discovery Using Natural Drugs as Substrates. Current Pharmaceutical Biotechnology 2003, 4, 153-167. ISSN: 1873-4316 (online) 1389-2010 (print) (Impact Factor 2.69) (9191 UGC notified journal)(web of science)
42. Keshetty S,Venisetty RK, Molmoori V and Ciddi V. Determination of Valdecoxib in Serum Using a HPLC Diode Array Detector and its Application in a Pharmacokinetic Study.Pharmazie 2006, 61(3), 245-246. ISSN: 0031-7144 (Impact Factor 0.96) (9827 UGC notified journal)(web of science)
43. Venkateswarlu K,Venisetty RK, Yellu NR, Keshetty S, PaiMG.Development of HPTLC - UV absroption densitometry method for the analysis of alprazolam and sertraline in combination and its application in the evaluation of marketed preparations. Journal of Chromatographic Sciences 2007, 45(8), 537-539. ISSN: 1945-239X (online) 0021-9665 (print) (Impact Factor 0.74) (19676 UGC notified journal)(web of science)
44. Venkateshwarlu K, Reddy YN, Srisailam K, Raj Kumar V and Pai MG. Determination of tramadol in capsules by high performance thin layer chromatography – densitometry.Current Trends in Biotechnology and Pharmacy, 2008, 2(3), 421-425. ISSN: 2230-7303 (online) 0973-8916 (print) (42 UGC notified journal)
45. Chitturi D, Venisetty RK, Molmoori RK, Kokate CK, Apte SS. Enhanced bioproduction of withaferin A from suspension cultures of Withaniasomnifera. Annals of Biological Research 2010, 1(2), 77-86. ISSN: 0976-1233
46. Kamarapu SK, Vaijayanthi, Bahlul ZEA and Venisetty RK. Development of RP-HPLC method for the analysis of levocetirizine and ambroxol hydrochloride in combination using PDA detector and its application in the evaluation of marketed preparations. International journal of Pharmaceutical sciences and Nanotechnology, 2010, 3(1),893-896.ISSN: 0974-3278 (43674 UGC notified journal)
47. Srisailam K, Raj Kumar V and Veeresham C. Predicting drug interaction of clopidogrel on microbial metabolism of diclofenac.Applied Biochemistry and Biotechnology, 2010, 160, 1508-1516. ISSN: 0273-2289 (Print) 1559-0291 (online) (Impact Factor 1.893) (3135 UGC notified journal)(web of science)

48. Aleti P, Venisetty RK and KamarapuSK.Development of RP-HPLC method for the analysis of Imatinibmesylate using PDA detector and its application in the evaluation of marketed preparations.International Journal of Pharmacy and Biological Sciences, 2011, 1(2), 14-18. ISSN: 2230-7605 (46322 UGC notified journal)
49. Venisetty RK, Keshetty S and Ciddi V. Biotransformation of Silibinin (Silybin) using fungal organisms. Indian Journal of Pharmaceutical Education and Research, 2011, 45(4), 384-391. ISSN: 0019-5464 (20841, 20842 UGC notified journal) (web of science)
50. M Jojula, RK Venisetty, MV Ramanama and SR Reddy. Isolation and Characterization of Mycobacterial Species in Clinically Diagnosed Cases of Pulmonary Tuberculosis and few associated with HIV Infections, Journal of Pure and Applied Microbiology, 2012, 6(3), 1415-1418. ISSN: 0973-7510. (19449 UGC notified journal) (web of science)
51. RK Venisetty and Kamarapu SK. RP-HPLC method development and validation for simultaneous estimation of clidinium bromide, chlordiazepoxide and dicyclomine hydrochloride in bulk and combined tablet dosage forms. International Journal of Advanced Biomedical & Pharmaceutical Research. 2013, 2(1), 35-40. ISSN: 2321-4961